

Reentry Phenomena Observed Using High-Frequency Radar

[Unclassified Title]

G. A. SKAGGS, C. B. TESAURO, AND F. H. UTLEY

*Radar Techniques Branch
Radar Division*

February 10, 1967



NAVAL RESEARCH LABORATORY
Washington, D.C.

CONTENTS

Abstract	ii
Problem Status	ii
Authorization	ii
INTRODUCTION	1
WSMR TEST OF AUGUST 4, 1965	1
GT-5 REENTRY OF AUGUST 29, 1965	4
SUMMARY	14
REFERENCES	14

ABSTRACT

The Madre radar has been deployed in an over-the-horizon mode to study reentry phenomena associated with Athena-boosted reentry experiments at the White Sands Missile Range and with reentering manned earth satellites of the Gemini type. Preliminary results indicate the feasibility of using hf radars for over-the-horizon detection of reentry bodies.

Examination of the results of a White Sands Missile Range reentry experiment demonstrates the advantage of velocity-time processing in the discrimination of multiple targets with various reentry characteristics. A cross-section assessment is made.

The analysis of the Gemini Titan-5 reentry makes available coarse capsule position information during reentry blackout at ranges beyond the line of sight. Measurable target cross sections are extracted. Approximate vehicle velocity may be determined from the doppler-time records. Real-time acceleration processing would allow detections of smaller target cross sections.

Reentry studies in the areas cited are continuing at the Naval Research Laboratory.

PROBLEM STATUS

This is an interim report on the problem; work is continuing.

AUTHORIZATION

NRL Problem R02-23
Project RF 001-02-41-4007
AF MIPR (30-602) 63-2928
AF MIPR (30-602) 63-2929
AF MIPR (30-602) 63-2995

Manuscript submitted November 3, 1966.

REENTRY PHENOMENA OBSERVED USING HIGH-FREQUENCY RADAR

INTRODUCTION

This report will discuss experimental results obtained with the Madre radar on two observations of reentry bodies. The Madre radar is a pulse doppler system utilizing cross-correlation, time-compression, narrow-band doppler processing techniques to improve signal-to-noise ratios in an hf over-the-horizon (OTH) mode of operation. The system is an adequate research tool for the detection of aircraft and missiles at extended OTH ranges.

For the two detections described in this report, target acquisition was achieved beyond the radar horizon. The next section of this report discusses the identification of multiple reentry elements for a White Sands Missile Range (WSMR) reentry experiment, and the following section is a discourse on the target characteristics of the Gemini Titan-5 (GT-5) during reentry. Estimates of reentry velocity and cross section are given.

WSMR TEST OF AUGUST 4, 1965

The purpose of the present reentry program at the WSMR is to deduce from simulated ICBM reentry configurations the characteristics of reentry bodies (REB), decoys, and chaff, at several frequencies, in order to establish discrimination criteria. NRL was invited informally to participate in OTH monitoring of the reentry phenomena. Such observations were initiated in July of 1965.

The experiments are reminiscent of NRL observations of NASA Trailblazer launches from Wallops Island, Virginia, in past years. The vehicle consists of two stages that accelerate the payload upward and two stages which accelerate the payload downward. The present launches are from Green River, Utah, with payload impact on the WSMR. The second, third, and fourth stages may all impact on the range, depending on the particular trajectory being flown. Two general trajectories are specified: one in which a low angle (20 degrees) of reentry is achieved with a peak altitude of 170 km and a reentry velocity of 20,000 ft/sec nominally; the second trajectory is one in which a 40-degree reentry angle is desired with apogee at 240 km and reentry velocity up to 23,000 ft/sec. Figure 1 shows an altitude vs time plot of a low-angle Athena-boosted trajectory for the launch of 4 August from Green River, Utah. The upper stages impact on the WSMR. The normal flight sequence calls for first- and second-stage separation before the payload and upper stages reach peak altitude. The first stage falls to earth within 50 mi of the Green River launch site. The second stage follows a ballistic trajectory to impact on the WSMR. The third stage accelerates the 4th stage and payload downward for approximately 30 sec and is separated shortly after engine cutoff. It then also assumes a ballistic trajectory until impact on the range. The fourth stage burns for 10 sec and further accelerates the payload downward. Within a second or two a retrorocket ignites, which separates the fourth stage from the payload. Both continue on slightly different earthbound reentry trajectories. Retrofire function for this flight occurred at 279.4 sec after launch at an altitude of 138 km.

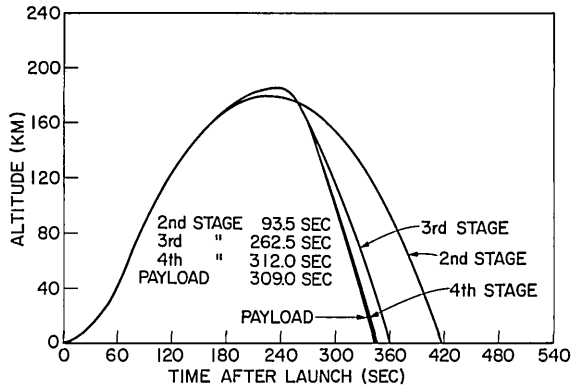


Fig. 1 - WSMR Athena trajectories for re-entry test of August 4, 1965 (Launch time $T_0 = 04:47:00$ GMT). Altitude in kilometers vs time after launch in seconds. Payload, 4th-stage, 3rd-stage, and 2nd-stage ballistic trajectories computed after times indicated on figure.

In lieu of complete postflight information for all stages, simple ballistic trajectories have been computed for the second, third, and fourth stages and the payload, beginning at the times indicated in the figure, i.e., second stage, 93.5 sec; third stage, 262.5 sec; fourth stage, 312 sec; and payload, 309 sec. No aerodynamic drag compensation has been included in the computation of reentry trajectories. If, in fact, the lower stages by being physically larger possess a higher drag coefficient, their impact times will be delayed somewhat from those indicated. This would make the differences in impact times of the payload and the other stages somewhat greater. On reentry at 70 km altitude the payload, which in this experiment passes at a reentry velocity of 21,000 ft/sec, leads the other stages by the following differences in time: fourth stage, 2 sec; third stage, 13 sec; and second stage, 64 sec. These separations in time would be increased depending on the aerodynamic lift or float characteristic of each stage. The radar operating parameters for the WSMR test of August 4, 1965, were as follows:

Radar frequency — 13.661 Mc/s

Pulse repetition frequency (prf) — 45 pps

Pulse width — 1.0 msec for \cos^2 pulse

Transmitter power — 4.6 MW peak, 90 kW average

Sensitive range interval — 1350 to 1800 naut mi

Minimum detectable cross section at 1600 naut mi — 50 m²

Backscatter coverage — 1310 to 1950 naut mi

Antenna, rotatable, on bearing of 265 degrees.

Figure 2 is a Doppler time history of the Madre results for the test. The ordinate is doppler frequency in cps and the abscissa is time in seconds after missile lift off (T_0). The displayed video is an intensity-modulated readout of doppler information sampled in a fixed-position constant-width range gate over a period of 7 min beginning at T_0 . The video analysis is accomplished through a predetection filter bandwidth of approximately 1 cps equivalent doppler width. This allows a 1-sec time resolution in the doppler time display. The range sample for this test was taken in a 20-naut mi range gate centered on

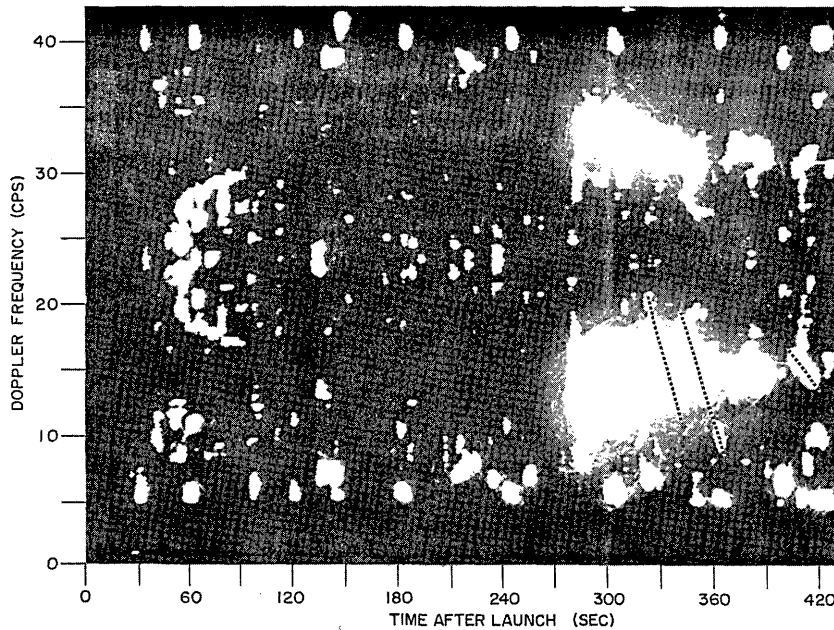


Fig. 2 - Doppler time history record for WSMR test of August 4, 1965. Doppler frequency (cps) vs time after launch in seconds for a 20-naut mi range gate centered on 1590 naut mi. Alternating black and white ribbons indicate discrete targets mentioned in text.

1590 naut mi. It should be noted that the video display is duplicated in a mirror symmetry above and below 22.5 cps doppler. This is due to the system operation on a prf of 45 pps. All doppler information becomes ambiguous for doppler frequencies separated by more than 22.5 cps from the rf carrier. It is desirable to consider only the video information below 22.5 cps, that above being redundant. There are several things of interest to be noted.

The first signal of interest occurs at a doppler frequency of 22 cps at $T_0 + 47$ sec and traces a diminishing doppler characteristic down to 16 cps at 92 sec. It is speculated that this signal might be the target return from the ballistic first stage of the Athena. First-stage separation occurred at $T_0 + 46$ sec. The signal onset seems to coincide quite well with the actual separation time. When the signal is acquired, the first stage is at an altitude of 28.6 km. The signal disappears 45 sec later when the first stage is at an altitude of 51 km. An attempt to compute the actual first-stage ballistic body doppler characteristic is being made but is not yet completed. A tentative cross-section assessment would indicate the echo to be less than 100 m^2 .

The next signal of note begins at $T_0 + 282$ sec over a spread of doppler frequencies from 8 to 18 cps. The doppler video envelope narrows in doppler width with increasing time until $T_0 + 390$ sec, at which time the video disappears at 14 to 15 cps. The onset of the broad, yet bounded doppler signal comes on the heels of the retrofire function which separates the 4th stage from the payload. Retrofire occurred at 279.4 sec at an altitude of 138 km. Signal onset came at 282 sec. The exhaust gas from the retrorocket possesses velocity components in excess of 30,000 ft/sec. It is speculated that retrorocket

exhaust gases, when allowed to diffuse through the upper E layer, generate a moving disturbance of modest echoing cross section. The possibility of such a reaction between the retrorocket exhaust gas volume and the ionospheric E region would certainly depend upon exhaust constituents and velocity, as well as on the ionospheric conditions existing near 120 km, such as quiescent ionization level, recombination rates, diffusion processes, and ionospheric wind characteristics. The mechanism for this multiple scatterer-type echo is not well understood. A definitive investigation is in process. Various echoing centers in the broad doppler signal evidence apparent cross sections ranging from 250 m² up to 1500 m².

Imbedded in the long-enduring signal are two discrete doppler lines which show decreasing doppler with increasing time. The first discrete signal begins at $T_0 + 311$ sec at a doppler frequency of 19.5 cps. It is believed that this echo corresponds to the re-entering payload fourth-stage complex which passes through an altitude of 75 km at $T_0 + 311$ to 313 sec. Doppler variations are taken directly from the photograph. The doppler variation with time is 0.6 cps². The diminishing doppler frequency is consistent with the deceleration that the incoming elements are subjected to, during reentry. The second discrete signal appears at $T_0 + 329$ sec at a doppler of approximately 18 cps. This agrees favorably with the third-stage trajectory which shows the third stage to be at 64 km at $T_0 + 329$ sec. The doppler rate of change with time is 0.4 cps². Both of these discrete doppler line signals yield cross sections of approximately 1000 m².

Another signal of shorter duration seems to be apparent at $T_0 + 398$ sec, beginning at a doppler frequency of 16 cps. This signal could quite likely be linked to the second stage. The time of intercept would put it at an altitude of 31 km based on the ballistic trajectory of Fig. 1. If, in fact, the second stage was a "floater," as the cw records of the Stanford Research Institute* (SRI) seem to indicate, acquisition would have come at a somewhat higher altitude. This would be consistent with reentry ionization phenomena. The apparent radar cross section of the second stage lies between 500 and 1000 m².

SRI has been active in observing the Athena reentry experiments in a cw bistatic mode. The Madre records and SRI's data for the test of August 4, 1965, (designated C014E03) have been compared, and notable agreement is found to exist in onset times for all signature components beginning with the wide doppler signal and including the payload fourth-stage complex, the third stage, and the second stage indications. Cross-section estimates are also in modest agreement. SRI has no data on the first-stage ballistic target.

In summary it can be concluded that reentry phenomena can be observed over the horizon, and that meaningful determinations can be made of slant range, velocity, and echoing cross section of reentry objects.

GT-5 REENTRY OF AUGUST 29, 1965

In continuing the discussion of reentry phenomena, it is appropriate to examine the preliminary analysis of Madre records for the earthward plunge of Gemini Titan-5, which was launched on August 21, 1965, and which reentered the earth's atmosphere on August 29, 1965. The Madre operating parameters for the GT-5 reentry were as follows:

*Private communication with Dr. David Johnson, SRI.

Radar frequency — 10.087 Mc/s
 Pulse repetition frequency (prf) — 90 pps
 Pulse width — 700 μ sec for \cos^2 pulse
 Transmitter power — 4 MW peak, 100 kW average
 Sensitive range interval — 400 to 850 naut mi
 Minimum detectable cross section at 450 naut mi — 500 m²
 Backscatter coverage — 570 to 950 naut mi and other hops
 Antenna, rotatable, on bearing of 215 degrees.

The principal mode of propagation to give illumination of the near approach of the GT-5 capsule and attendant ionization sheath or trail was via one-hop E-layer refraction, with the effective refractive layer height being 145 km. All reentry characteristics have been deduced from NASA postflight material obtained from the Goddard Space Flight Center,* Greenbelt, Md.

Figure 3 is a plot of ground range and slant range vs time. Both range estimates have been computed relative to the Chesapeake Bay Madre site. It is to be noted from the curves that the point of nearest approach occurred roughly midway between 1245:30 GMT and 1246:00 GMT.

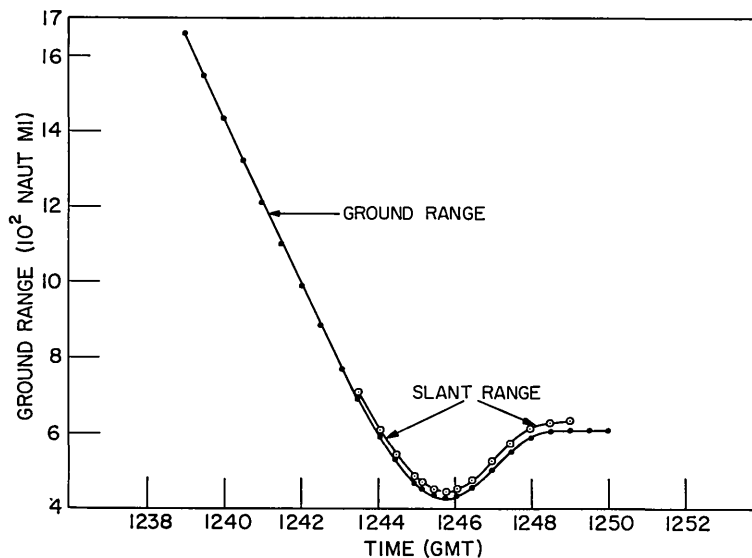


Fig. 3 - Gemini Titan-5 reentry ground range and slant range (naut mi) vs time (GMT). The ground and slant ranges to the target are computed from earth track and via 145-km E-layer refraction, respectively, to the Chesapeake Bay MADRE installation of NRL.

*Mr. Jerry Barsky of Goddard has made GT postflight data available to NRL.

Figure 4 traces out the bearing angle of the capsule referenced to the Chesapeake Bay Division (CBD) site for GMT times from 1238:15 to 1250:00. The horizontal lines that intersect the curve indicate the two-way 3-db coverage of the rotatable antenna as positioned. It is to be noted that the rate of change of bearing angle is the greatest between 1245 and 1246 GMT. The magnitude of the rate of change is 30 degrees in 60 sec, or 0.5 degree per sec.

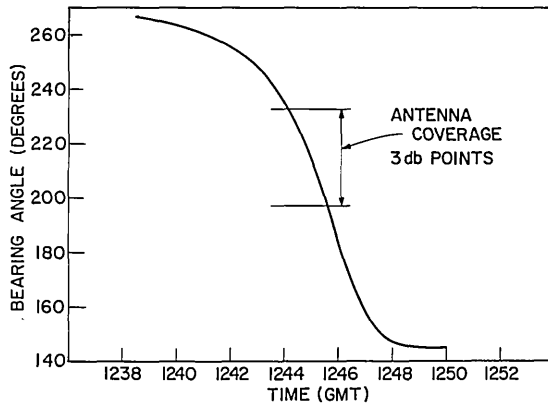


Fig. 4 - Gemini Titan-5 reentry bearing angle (degrees) vs time (GMT) referenced to CBD

Figure 5 is a plot of the doppler frequency of the GT-5 capsule vs time. It is computed on the basis of a 10.087-Mc/s operating frequency and 145-km refracting layer height. It should be particularly noted that the doppler frequency has been allowed to fold at the point at which it passes through zero cps. Actually, the doppler frequencies plotted before the zero frequency crossover are above the carrier frequency, corresponding to an approaching target, while those dopplers plotted after the zero crossover are below the carrier frequency and correspond to the returns from a receding target. The original Madre signal processing techniques allowed for both approach and recede target dopplers to be folded together at a zero frequency *i-i*. Doppler sense can be easily restored with the offsetting of receiver reference frequencies and also by preserving doppler bandwidths of interest through separate approach and recede detection circuits. For the purpose of the GT-5 experiment, the Madre processor was allowed to fold the approach and recede target spectrums. From Fig. 5 it can be seen that the doppler frequency goes to zero shortly after 1245:45. The actual time is 12:45:48 GMT.

Figure 6 is a plot of folded doppler frequencies vs time. Figure 5 only manifested one doppler fold whereas Fig. 6 shows multiple folds. This abundance of folds in doppler frequency is due to pulsed operation at a prf of 90 pps, which makes all dopplers ambiguous when removed by more than 45 cps from the radar operating frequency. The doppler frequency to be analyzed is seen to fold at multiples of 45 cps. From 1244 to 1248:30 GMT the Gemini capsule doppler frequency sustains 16 folds either at zero cps or at 45 cps.

Figure 7 is an expanded plot of part of Fig. 6 with the times of signal onset and signal termination indicated. The doppler time plot is boxed in for the interval of time during which the capsule ionization was detected. The echo was larger than the minimum detectable signal for 31 sec from 1245:28 to 1245:59. The cross-hatched portion of the curve from 1245:37 to 1245:46 has been analyzed for echoing cross-section and velocity assessment.

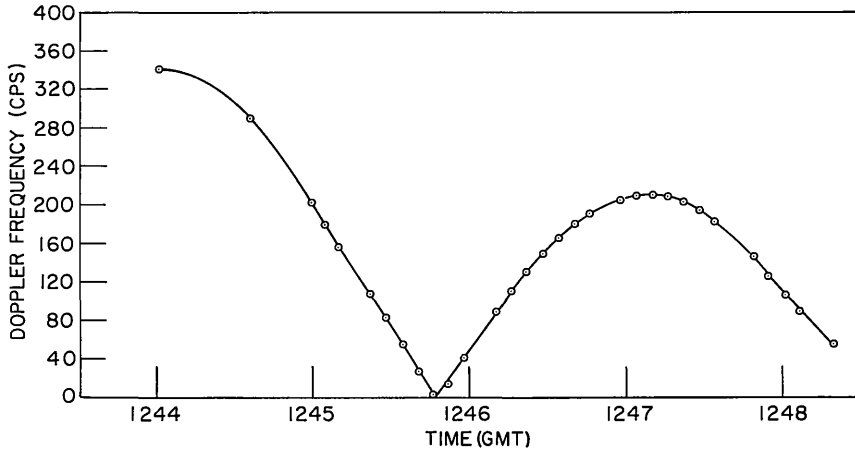


Fig. 5 - Gemini Titan-5 reentry doppler frequency (cps) vs time (GMT) as referenced to CBD. The approach and recede velocities are folded at broadside aspect angle.

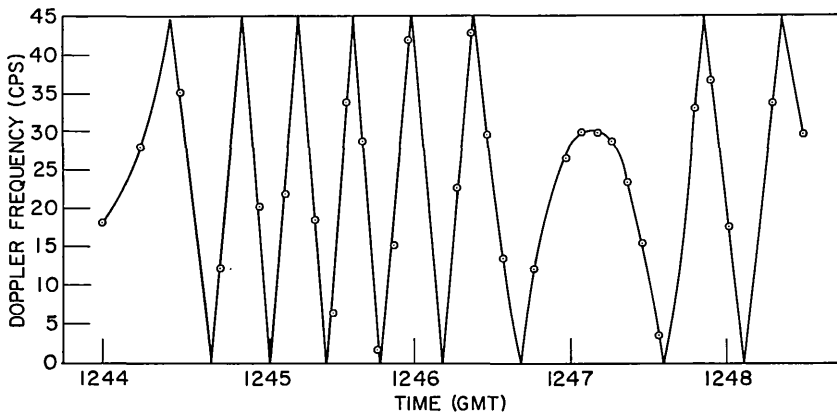


Fig. 6 - Gemini Titan-5 reentry folded doppler frequency (cps) vs time (GMT) as referenced to CBD. The abundance of folds is due to pulsed operation at a prf of 90 pps.

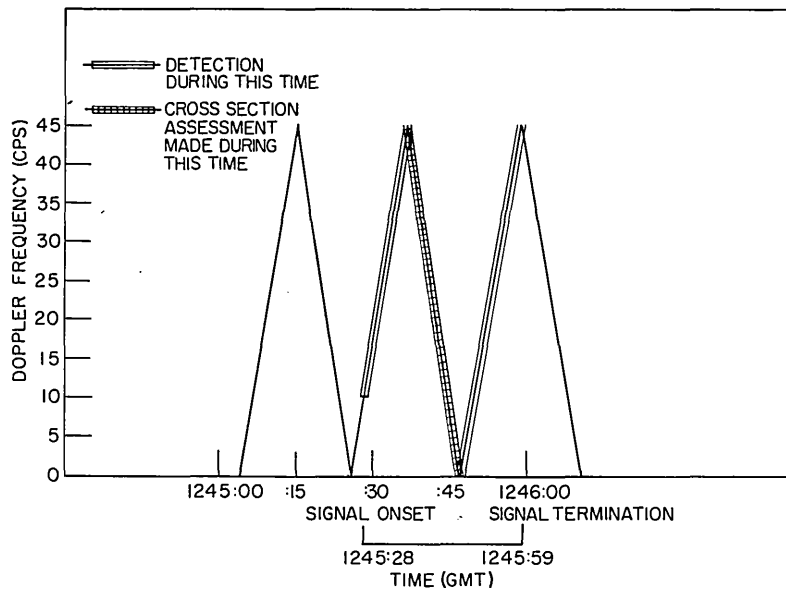


Fig. 7 - Expanded plot of part of Fig. 6 showing detection times (GMT) for GT-5 reentry folded Doppler frequency (cps). The boxed-in portion of the plot is for the interval of time during which the capsule ionization was detected. The cross-hatched portion has been analyzed for echoing cross-section and velocity assessment.

Figure 8 is a 2-min doppler time history display of Madre results for the GT-5 reentry. The ordinate is doppler frequency in cps. The abscissa is time in seconds after 1245:00 GMT with the modification that the displayed video has been expanded 2:1 along the time scale. Unfortunately, the time scale has not been corrected, so the following time correspondence is in order:

1245:00 GMT = 0 sec on abscissa
 1245:30 GMT = 60 sec on abscissa
 1246:00 GMT = 120 sec on abscissa
 1246:30 GMT = 180 sec on abscissa
 1247:00 GMT = 240 sec on abscissa.

The video information displayed in Fig. 8 was processed from a 2-min store of range-gated doppler samples. The range gate was 20 naut mi in width and was centered at a slant range of 450 naut mi. The Madre radar horizon for line-of-sight detection is 90 km for a 450-naut mi range. The GT-5 was acquired at an altitude of 76.3 km and observed down to 67.4 km. The altitude of detection varies from 14 to 20 km below the radar horizon. Detection is apparent in Fig. 8 from 1245:37 to 1245:55 GMT. The range gate centered on 470 naut mi indicated signals above noise for the times 1245:28 to 1245:37 GMT and also from 1245:55 to 1245:59 GMT. The doppler time analysis for the range gate centered on 470 naut mi is not presented.

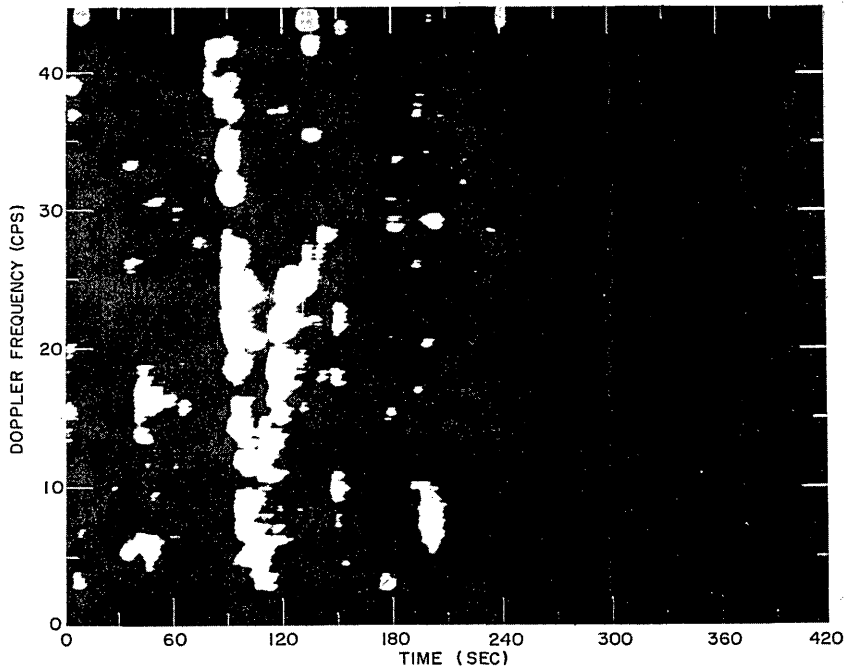


Fig. 8 - Gemini Titan-5 reentry doppler time history record showing doppler frequency (cps) vs time (GMT) on August 29, 1965. Two-minute record beginning at 12:45:00 for a 20-naut mi range gate centered on 450 naut mi. The video display has been expanded 2:1 in time. The seconds enumerated on the abscissa should be halved; 60 sec is 1245:30, 120 sec is 1246:00, 180 sec is 1246:30, and 240 sec is 1247:00 GMT

The target signal shows signs of moderately strong scintillation in echo strength. An exact analysis to determine the degree of periodicity of the scintillation has been performed. Correlation of this analysis with reentry phenomena has not been accomplished. NASA* has advised that the GT-5 capsule had a roll rate of 20 degrees per sec during reentry, which would not account for any fast variations. The fluctuations in signal strength may be due in part to ionospheric path anomalies. The detected signal traces out very well the actual capsule velocity-time relationship. An estimate of capsule velocity can be derived if the range of nearest approach is known. In this case the nearest approach was determined to be 450 naut mi. The following equation can be used to compute the spacecraft velocity at the time of nearest approach:

$$v^2 = \frac{R_0 \lambda (df/dt)_{max}}{2}$$

where

*Private communication with Mr. Leon Woldorff of NASA.

V = velocity of manned satellite

R_0 = range of closest approach

λ = operating wavelength

$(df/dt)_{max}$ = the maximum rate of change of the doppler frequency with time.

For the display of Fig. 8 the best time resolution is of the order of 1 sec. In order to measure $(df/dt)_{max}$ it is necessary to determine the 45-cps and zero-cps crossover of the descending doppler line. With diligence, the time difference between the 45-cps and zero-cps crossing was determined by two observers. The two time differences were 10 sec and 11 sec. Both were used to compute a $(df/dt)_{max}$, and then two separate solutions were computed for the capsule velocity. As an equally likely, or perhaps better, estimate, the average between 10 and 11 sec, namely 10.5 sec, was used to determine $(df/dt)_{max}$ and also V . The various solutions are shown below:

$R_0 = 450$ naut mi (converted to feet)

$\lambda = 91$ ft (for frequency of 10.087 Mc/s)

$(df/dt)_{max} = 45/10, 45/11, \text{ and } 45/10.5.$

For $(df/dt)_{max} = 45/10$, $V = 24,550$ ft/sec; for $45/11$, $V = 23,400$ ft/sec; and for $45/10.5$, $V = 23,980$ ft/sec.

As can be seen from the comparison of velocities as determined with three different values of $(df/dt)_{max}$, good time resolution is necessary for an accurate estimate of velocity. The difference is 500 ft/sec or more for each difference in time of 0.5 sec. The velocity isn't modified quite so critically for small changes in R_0 , the range of nearest approach. A difference of 1 naut mi changes the velocity estimate by 30 ft/sec, and a difference of 10 naut mi alters the velocity by 300 ft/sec. The velocity given in the NASA postflight data for the time of closest approach was 23,996 ft/sec. This compares very well with the above determinations.

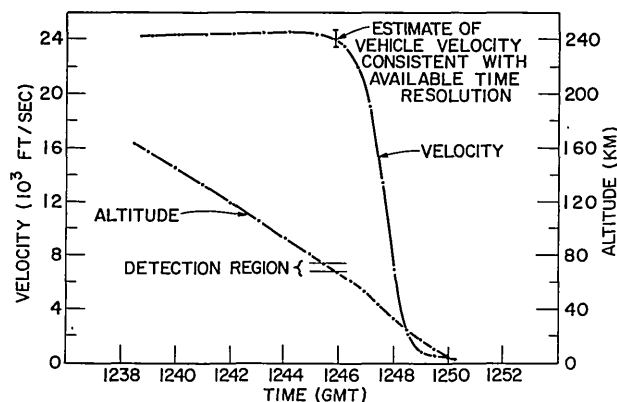


Fig. 9 - Gemini Titan-5 reentry altitude (km) and velocity (ft/sec) vs time (GMT)

A brief look at Fig. 9 will show the point on the velocity-time curve where the above velocity estimate was made. Also plotted in Fig. 9 is the altitude-time history of the re-entry trajectory. The Madre detection covers the altitude region from 73.6 km down to 67.4 km.

Table 1 is a summary of cross-section estimates made on the descending line of the signal video in Fig. 8. In order to get the display of Fig. 8, time-stored range-gated doppler samples which were stored for 2 min were analyzed through a quite broad (1-cps) doppler bandwidth predetection filter in order to enhance time resolution. In order to make the cross-section measurements recorded in Table 1, the same stored signal information is processed through a predetection bandwidth of 0.1-cps equivalent doppler bandwidth. This allows amplitude information to be read out as the 40-cps (5 to 45 cps) doppler information is strobed 0.1 cps at a time. Doppler analysis from 0 to 5 cps is precluded by Madre clutter filters. Amplitude samples have been taken at various points along the negative sloped video trace. These amplitudes have been compared to a system calibration signal for proper cross-section assessment. Table 1 shows the cross sections determined for various doppler frequencies.

Table 1
Apparent Radar Cross Section for
Various Doppler Frequencies

Frequency (CPS)	Cross Section* (M ²)	
	System Compensation Only	System and Path Loss Compensation
40.2	2×10^3	2×10^4
34.8	3.2×10^3	3.2×10^4
28.2	4.5×10^3	4.5×10^4
23.8	9.6×10^3	9.6×10^4
20.4	1.4×10^4	1.4×10^5
15.4	2.6×10^4	2.6×10^5
12.3	4.7×10^4	4.7×10^5
11.0	1.6×10^5	1.6×10^6
9.6	2.4×10^5	2.4×10^6
8.4	2.4×10^5	2.4×10^6
5.3	4.5×10^5	4.5×10^6

*Minimum detectable cross section = $5 \times 10^2 \text{ m}^2$.

The system compensation mentioned consists of three adjustments which are as follows:

Lack of illumination —

- | | |
|---|-------|
| 1. Target out of vertical beam, two-way loss: | 16 db |
| 2. Target out of horizontal beam, two-way loss: | 4 db |
| Antenna bearing: 215° bearing | |
| Target intercept: 191° bearing | |

Processing loss —

- | | |
|---|-------|
| 3. Signal not of constant velocity; target echo velocity-time characteristic of 4.2 cps ² mismatched with processor bandwidth of 0.1 cps; approximate mismatch loss: | 16 db |
|---|-------|

System loss (compensation)	36 db
----------------------------	-------

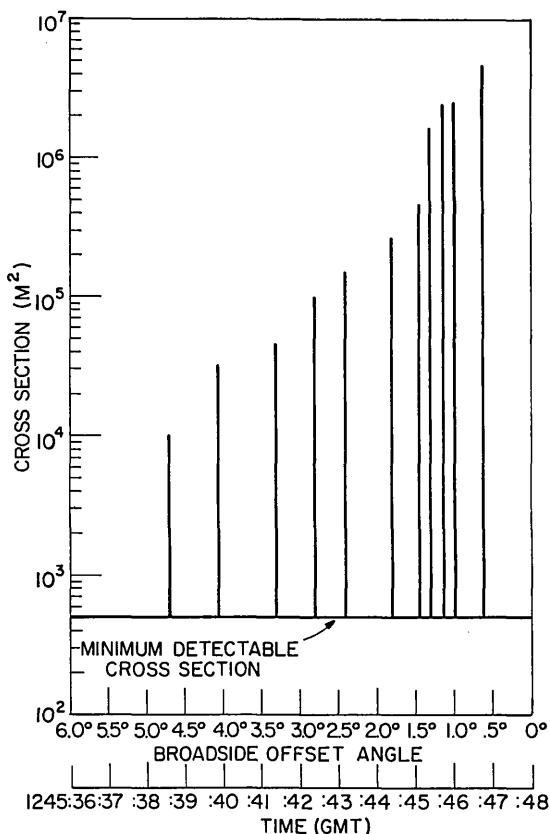
The path loss of 10 db which was used was a modest estimate based on one-hop E-layer propagation data from the National Bureau of Standards, Central Radio Propagation Laboratory (1), predictions for a sunspot number of 10.

It can be seen that the target cross section increases as the doppler frequency is diminished. The maximum cross section listed under system and path loss compensation is 4.5×10^6 square meters. This could be larger or smaller depending on the path loss assumed. Lin (2) reported a cross section of 1.6×10^6 m² for the MA-6 at an altitude of 67 km.

It might be remembered that Fig. 4 indicated that the bearing angle to the capsule was changing more rapidly as the capsule neared its closest approach to the radar and then moved away. The highest rate of bearing variation was 30 degrees in 60 sec, or 0.5 degree per sec. If it took 10 sec, for instance, for the capsule doppler to go from 45 cps to zero cps, then the aspect angle would have changed by 5 degrees, so it would be possible to plot target cross section against what has been called broadside offset angle, which is actually the angle by which the capsule and its trail fail to be perpendicular to the radar ray. Figure 10 is such a plot showing cross section, in square meters, as the ordinate and broadside offset angle and time (GMT) on the abscissa. The large minimum detectable cross section of 500 m² is due to the target appearing off the antenna beam bearing and in an appreciable vertical pattern null. It appears as if the cross section is aspect sensitive to the extent of 2-1/2 orders of magnitude in a little more than 4 degrees of angle change. As mentioned earlier the existing clutter filters of the Madre system precluded a cross-section assessment at zero degrees offset. McKinley (3) and Manning (4) both indicate that meteor reflections are highly specular and extremely aspect sensitive. A few degrees either side of the right-angle geometry eliminates the echo return. Lin (2) indicates by his results an aspect sensitivity of approximately 1-1/2 orders of magnitude for an angular change of 10 degrees.

In reviewing Madre results for other Gemini reentries (GT-3, 4, 6, and 7) two things seem to be reasonably consistent: first, the target echoing area increases by at least an order of magnitude, and perhaps two, at the point of perpendicular crossing, and second, the altitude of onset of signal seems to be similar for the several reentries. The viewing

Fig. 10 - Gemini Titan-5 apparent radar cross section (m^2) vs broadside offset angle (degrees) and time (GMT)



geometry for the Madre equipment is virtually the same for each reentry, namely broadside to the trajectory. The altitude of onset might be expected to be constant, or nearly so, because of the similarity in reentry velocities. Lyon (5) et al. reported at the ARPA meeting of July 7-8, 1965, that they had acquired the GT-3 at an altitude of 82 km. The WSMR experiment described earlier demonstrated that reentry bodies with velocities of approximately 21,000 ft/sec present enhanced cross sections below an altitude of 80 km. In order to see the maximum enhanced target cross section it appears necessary to illuminate the predicted reentry corridor over a particular altitude regime, which may be narrow, and also to engage the trajectory at the proper aspect angle.

Lowe (6) of RCA has examined the feasibility of using hf surveillance and tracking for the Apollo reentry. In addition to his suggestions, it is recommended that such a system not depend on enhanced targets for detection but rather have a skin track capability. It seems probable that the Apollo spacecraft will not generate several orders of magnitude enhancement of its cross section due to trail ionization on its first penetration into the earth's atmosphere, if that penetration is constrained to be no lower than 110 km. The altitude at which the Apollo will generate an enhanced cross section will depend on its second-entry velocity.

SUMMARY

It has been shown that velocity-time processing can provide sufficient discrimination to study reentry vehicles at OTH ranges. The Madre results on GT-5 show that a matched velocity-time processor (acceleration filter) would allow a 16-db improvement in S/N.

It is recommended that Apollo surveillance systems be designed to include skin track capability as well as real-time acceleration processing.

REFERENCES

1. Lucas, D.L., "The Role of Ionospheric Predictions in the Geographic Location of OHD Systems," (Stanford Research Institute Report SRI-5-1786, pp. 7-19 (Unclassified Title, Secret Report)), ARPA OHD meeting of July 7-8, 1965; Proc. ARPA OHD
2. Lin, Shao-Chi, "Radio Echoes from a Manned Satellite during Re-Entry," J. Geophys. Res. 67:3851 (Sept. 1962)
3. McKinley, D.W.R., and Millman, P.M., "A Phenomenological Theory of Radar Echoes from Meteors," Proc. IRE 37:364 (Apr. 1949)
4. Manning, L.A., and Eshleman, V.R., "Meteors in the Ionosphere," Proc IRE 47:186 (Feb. 1959)
5. Lyon, E., Bowserc, A., and Lee, J.D., "Observations of a Reentering Body," (Stanford Research Institute Report SRI-5-1786, pp. 281-303 (Unclassified Title, Secret Report)), ARPA OHD meeting of July 7-8, 1965; Proc. ARPA OHD
6. Lowe, M. H., "H. F. Applications to Command Capsule Reentry Surveillance and Tracking," presented at IEEE Convention, Session 67, March 24, 1966

DOCUMENT CONTROL DATA - R & D

(Security classification of title, body of abstract and indexing annotation must be entered when the overall report is classified)

1. ORIGINATING ACTIVITY <i>(Corporate author)</i> Naval Research Laboratory Washington, D.C. 20390		
3. REPORT TITLE <i>(Unclassified)</i> REENTRY PHENOMENA OBSERVED USING HIGH-FREQUENCY RADAR		
4. DESCRIPTIVE NOTES <i>(Type of report and inclusive dates)</i> An interim report on the problem		
5. AUTHOR(S) <i>(First name, middle initial, last name)</i> Skaggs, G.A., Tesauro, C.B., and Utley, F.H.		
6. REPORT DATE February 10, 1967	7a. TOTAL NO. OF PAGES 18	7b. NO. OF REFS 9
8a. CONTRACT OR GRANT NO. NRL Problem R02-23	9a. ORIGINATOR'S REPORT NUMBER(S) NRL Report 6507	
b. PROJECT NO. RF 001-02-41-4007 and		
c. AF MIPR (30-602) 63-2928 AF MIPR (30-602) 63-2929		
d. AF MIPR (30-602) 63-2995	9b. OTHER REPORT NO(S) <i>(Any other numbers that may be assigned this report)</i> None	
10. DISTRIBUTION STATEMENT		
11. SUPPLEMENTARY NOTES None	12. SPONSORING MILITARY ACTIVITY Department of the Navy (Office of Naval Research) and Dept. of the Air Force	
13. ABSTRACT <p>The Madre radar has been deployed in an over-the-horizon mode to study re-entry phenomena associated with Athena-boosted reentry experiments at the White Sands Missile Range and with reentering manned earth satellites of the Gemini type. Preliminary results indicate the feasibility of using hf radars for over-the-horizon detection of reentry bodies.</p> <p>Examination of the results of a White Sands Missile Range reentry experiment demonstrates the advantage of velocity-time processing in the discrimination of multiple targets with various reentry characteristics. A cross-section assessment is made.</p> <p>The analysis of the Gemini Titan-5 reentry makes available coarse capsule position information during reentry blackout at ranges beyond the line of sight. Measurable target cross sections are extracted. Approximate vehicle velocity may be determined from the doppler-time records. Real-time acceleration processing would allow detections of smaller target cross sections.</p> <p>Reentry studies in the areas cited are continuing at the Naval Research Laboratory.</p>		

14. KEY WORDS	LINK A		LINK B		LINK C	
	ROLE	WT	ROLE	WT	ROLE	WT
Radar Reflections Reentry Vehicles Radar Targets Radar Signals High Frequency Processing Ionospheric Propagation Ionization Trails Target Discrimination Radar Cross Sections Over-the-Horizon Detection						